Int. J. Multiphase Flow Vol. 17, No. 3, pp. 327–342, 1991
Printed in Great Britain

0301-9322/91 $3.00 + 0.00
Pergamon Press/Elsevier

TWO-PHASE FLOW PATTERNS AND TRANSITIONS IN A SMALL, HORIZONTAL, RECTANGULAR CHANNEL

M. W. WAMBSGANSS,[1] J. A. JENDRZEJCZYK[1] and D. M. FRANCE[1,2]

[1]Materials and Components Technology Division, Argonne National Laboratory, Argonne, IL 60439, U.S.A.

[2]Department of Mechanical Engineering, University of Illinois at Chicago, M/C 251, P.O. Box 4348, Chicago, IL 60680, U.S.A.

(Received 17 July 1990; in revised form 11 November 1990)

Abstract—Horizontal two-phase flow was studied in a small cross-sectional-area (19.05 × 3.18 mm) rectangular channel with both the short and long sides forming the base, resulting in aspect ratios of 6 and 1/6, respectively. Adiabatic flows of air/water mixtures were tested over a large mass flux range (50–2000 kg/m² s). The full quality range was considered whenever experimentally achievable. Flow patterns were established and both mean and dynamic pressure measurements were used to accurately establish the plug/bubble-to-slug flow transition. This result, together with visual observations and supplemented with photographic data, was used to develop flow pattern maps. A comparison of existing flow pattern maps for circular pipes, capillary tubes and larger rectangular channels led to the conclusion that, while qualitative agreement exists, these maps are not generally applicable to the subject small rectangular channel on the quantitative basis.

Key Words: two-phase flow, horizontal, rectangular, flow patterns, transitions

INTRODUCTION

Heat transfer to single-phase fluids in compact heat exchangers has been studied extensively for a variety of applications. The use of such exchangers for two-phase fluids has, however, received much less attention. The phenomenon of two-phase flow in a channel, whose characteristic dimension may be smaller than a typical bubble diameter, is intriguing and must be addressed separately for this application. Although numerous results exist in the engineering literature pertaining to two-phase flows in large-diameter channels, size and geometry are significantly different in the case of interest. A horizontal rectangular channel with small cross-sectional area was used in this study as representative of the flow passages in plain-fin compact heat exchangers.

As suggested in Hosler (1968), knowing the flow pattern in two-phase flow is analogous in single-phase flow to knowing whether the flow is turbulent or laminar. The importance of knowing flow patterns in the design of heat exchangers is the theme of a recent paper by Bell (1988). Knowledge of the flow patterns allows one to apply an appropriate fluid-dynamic or heat transfer theory. As emphasized in the state-of-the-art reviews of Shah (1982) and Westwater (1986), knowledge of two-phase flow patterns is essential in design.

Two-phase flow in circular tubes has been studied by numerous investigators over the last 40 years. Both vertical and horizontal orientations, as well as inclined orientations, have been studied. Flow patterns have been identified and the transitions between flow patterns have been defined, primarily from visual observations. As such, the determination is somewhat subjective. Furthermore, it must be recognized that in most cases the transitions between flow patterns, as defined on flow pattern maps, are not "sharp lines", but rather, fairly wide bands with the transition occurring gradually as the band is traversed. Attempts have also been made to develop predictive methods for flow pattern transitions based on information derived from pressure and/or void fraction fluctuations (e.g. frequency spectra).

Horizontal flow patterns are controlled by gravity and vapor shear forces: gravity forces dominate at low flow velocities corresponding to stratified and wave flow; vapor shear forces dominate at high flow velocities corresponding to annular flow. A third force, that associated with surface tension, can be important in very small channels.

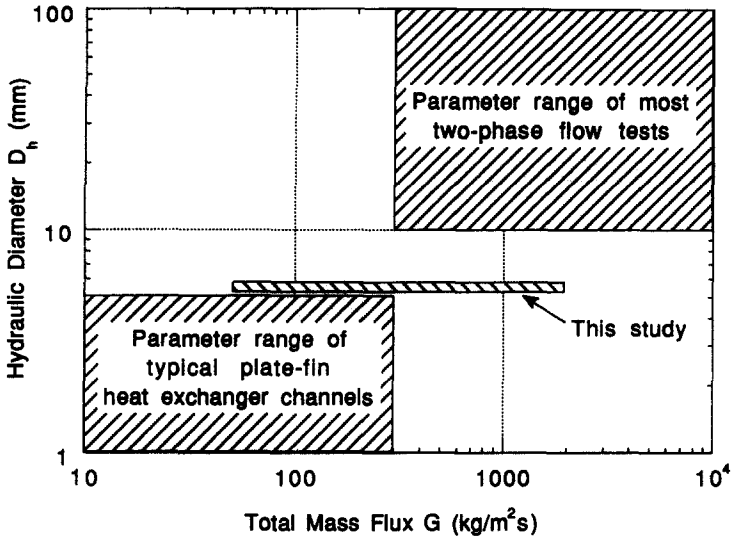

Figure 1. Data parameter ranges.

The majority of previous two-phase flow pattern studies have involved circular tubes, with diameters on the order of 10–75 mm, tested at mass velocities >300 kg/m^2 s. [While there have been some studies of two-phase flow in large-diameter conduits (200–300 mm), there have been relatively few studies at very small diameters.] Plate-fin heat exchangers, on the other hand, typically have flow passages with equivalent (hydraulic) diameters in the range 1–10 mm and operate with mass velocities in the range 10–300 kg/m^2 s. These two flow situations are illustrated schematically in figure 1. It is noteworthy that, in the parameter range for plate-fin heat exchanger channels, the flow regime corresponding to the liquid flowing alone in the channel will always be *laminar*.

Studies of two-phase flow patterns in rectangular channels, listed in table 1, cover a period of more than 30 years. Flow channel sizes are given in the table; all are larger than the channel in this study. Fluids employed, aspect ratio and channel orientation are also included in table 1. The following is a discussion of these studies on an individual basis. Selected results from these studies will be compared subsequently with results from the present investigation.

Richardson (1958) investigated the behavior of air/water mixtures in horizontal rectangular channels. He utilized three different channels, as given in table 1. The channels were oriented so

Table 1. Two-phase flow pattern experiments with rectangular channels (geometries/mixture/test condition)

Investigator(s)	Channel cross-section (mm)	D_h (mm)	Aspect ratio,[a] β	Orientation	Fluid mixture	Test condition
Richardson (1958)	6.35 × 50.8	11.3	0.125	H	Air/water	Adiabatic
	12.7 × 50.8	20.3	0.250	H	Air/water	Adiabatic
	25.4 × 50.8	33.9	0.50	H	Air/water	Adiabatic
Hosler (1968)	25.4 × 3.14	5.68	8.0	V	Steam/water	Heated
Jones & Zuber (1975)	63.5 × 5.0	9.27	12.7	V	Air/water	Adiabatic
Troniewski & Ulbrich (1984)	51.1 × 4.6	8.40	11.2	V, H	Air/water	Adiabatic
	42.1 × 4.4	7.97	9.7	V, H	Air/water	Adiabatic
	37.8 × 4.7	8.36	8.1	V, H	Air/water	Adiabatic
	30.1 × 6.4	10.56	4.7	V, H	Air/water	Adiabatic
	22.6 × 7.85	11.65	2.9	V, H	Air/water	Adiabatic
	18.9 × 9.6	12.73	2.0	V, H	Air/water	Adiabatic
	12.7 × 13.5	13.09	0.94	V, H	Air/water	Adiabatic
	9.9 × 18.8	12.97	0.53	V, H	Air/water	Adiabatic
	6.0 × 29.5	9.97	0.20	V, H	Air/water	Adiabatic
	4.1 × 41.5	7.46	0.099	V, H	Air/water	Adiabatic
Lowry & Kawaji (1988)	80 × 0.5	0.5[b]	160	V, H	Air/water	Adiabatic
	80 × 1.0	1.0[b]	80	V, H	Air/water	Adiabatic
	80 × 2.0	2.0[b]	40	V, H	Air/water	Adiabatic

[a]Vertical orientation: β = long side/short side. Horizontal orientation: β = height/base.
[b]Characteristic length dimension taken to be spacing between plates.

that the long side of the rectangle formed the base, i.e. was horizontal. Consequently, the aspect ratios, when defined as the ratio of the height of the channel to the base, were <1 (table 1). Richardson presented a flow pattern map for each of the three channels tested. Small channel heights minimized the occurrence of stratified and wave flows due to the ease with which liquid reached the top of the channel and gave rise to slug, plug or bubbly flows.

Hosler (1968) reported results of a study to determine the flow patterns existing in two-phase flow in a narrow rectangular channel (table 1) with heat addition to boil water at high pressure (2–14 MPa). The test section was vertically oriented, and the flow was directed upward.

Hosler identified three primary flow regimes: bubble flow, slug flow and annular flow. He concluded that *the flow patterns observed in boiling flow appear similar to flow patterns observed in adiabatic flow*. System pressure was shown to have a significant effect on the flow patterns. In particular, as the pressure is increased the bubble size decreases, and the transitions from bubble to slug and slug to annular occur at higher local qualities.

Jones & Zuber (1975) studied vertical upflow of air/water mixtures in a rectangular channel. Their objective was to evaluate the interrelationship between void fraction fluctuations (as sensed by a linear X-ray void measurement system) and flow patterns. The flow channel was formed from lucite plates; the channel dimensions are given in table 1. Air(water) was injected into the main stream of water(air) through porous stainless steel plates in the sides of the channel. The authors presented photographs of the various flow patterns observed.

Jones & Zuber (1975) stressed the "variable nature of some regions of flow". For example, they noted that in slug flow "... there frequently occurs a chaotic, twisting conglomeration of liquid and gas. The major bubbles in slug flow invariably oscillate wildly from side to side and snakewise along their length". They stated that the results showed a definite von Karman vortex street behavior by the entrained bubbles behind the major voids; the vortex street behavior was suggested to be the result of liquid flowing past the elongated voids. Also, the annular flow pattern was not well-defined. Rather, Jones & Zuber reported "small ripples and large waves" giving rise to "frothy slugs". In general, *the flow situations inherent in the slug and annular flow patterns are distinctly heterogeneous. The bubbly flow pattern, on the other hand, is well-defined.*

Troniewski & Ulbrich (1984) studied 10 different rectangular channels with aspect ratios ranging from 12 to 0.1; the channel dimensions are given in table 1. Investigations were carried out in vertical channels with aspect ratios in the range 1–12 and in horizontal channels with aspect ratios in the range 0.1–10. The majority of the tests used air/water, and selected tests employed aqueous solutions of sugar/air mixtures in order to study the effect of viscosity.

As a result of their research, Troniewski & Ulbrich (1984) proposed flow pattern maps for both vertical and horizontal two-phase flows in rectangular channels. The channels for horizontal flow were divided into "rectangular" and "crevice" channels. Crevice channels were distinguished from rectangular channels by the fact that the vertical dimension of the crevice channel (in the direction of the force of gravity) was very small; for this group of channels, stratified and wavy flow regimes were not found. Experiments with aqueous solutions of sugar/air mixtures led to the conclusion that *liquid viscosity (up to 0.040 kg/m^2 s) has an insignificant effect on the flow pattern transitions.*

Lowry & Kawaji (1988) studied flow patterns associated with vertical upflow of air/water through narrow channels formed by two flat plates; see table 1 for channel dimensions. Flow patterns were observed photographically with a strobe flash, and flow pattern maps were developed for the two narrowest gaps. Transition boundaries could not be determined without ambiguity for the smallest (0.5 mm) gap.

The flow pattern transitions observed by Lowry & Kawaji (1988) were compared with the transitions predicted by the correlations of Taitel *et al.* (1980), which were developed for flow in circular pipes of moderate to large diameter. Lowry & Kawaji (1988) concluded that the *pipe correlations of Taitel et al. are not valid for narrow channels*; in particular, they noted that the transition to annular flow was predicted to be independent of superficial liquid velocity, while the maps showed dependent behavior. Lowry & Kawaji (1988) developed a new model for the transition to annular flow. The *need for additional data for a wider range of velocities and gap widths and for different liquid viscosities and surface tensions was emphasized.*

The results presented in this study are from a two-component (air/water), two-phase flow in a horizontal channel (19.06 × 3.59 mm) (Wambsganss *et al.* 1990). The channel can be considered

to represent the upper limit on flow passage size found in plate-fin heat exchangers; see figure 1. Two orientations were studied: long sides of the rectangle oriented vertically (aspect ratio of 6) and horizontally (aspect ratio of 1/6). Flow patterns were determined over a relatively large range of total mass flux ($50 < G < 2000\ \mathrm{kg/m^2\,s}$) in order to include all flow patterns typically found in larger channels. The experiments were adiabatic and used a two-component mixture of air and water; special attention was given to the transitions between patterns. In the course of this work, visual and photographic observations were used. Mean and dynamic pressure measurements served to refine transition definition. Detailed flow pattern definitions were coupled to photographs that included variations within specific flow patterns. Flow pattern maps are presented, and the applicability of existing maps for circular pipe flow and larger rectangular channels was evaluated. In particular, comparisons were made with results from larger-diameter circular channels, smaller-diameter circular channels in the capillary tube range and larger rectangular channels.

EXPERIMENTAL APPARATUS

The flow apparatus was designed to allow adiabatic flow experiments with air/liquid mixtures in channels of small cross-sectional areas. The apparatus is illustrated schematically in figure 2. Air is supplied from a compressed air storage tank and flows through a pressure regulator and preselected rotameter to an air/liquid mixer. The liquid flows through a control valve and preselected rotameter to the mixer. In the mixer, air is injected into the liquid stream through a porous medium located in opposing walls of the flow channel. The two-phase mixture then flows through the transparent channel to a drain. Domestic water was the liquid used in this study; however, the apparatus shown in figure 2 is capable of operating as a closed circuit for use with non-expendable fluids. A bellows-type dry gas meter was utilized to calibrate the gas rotameters,

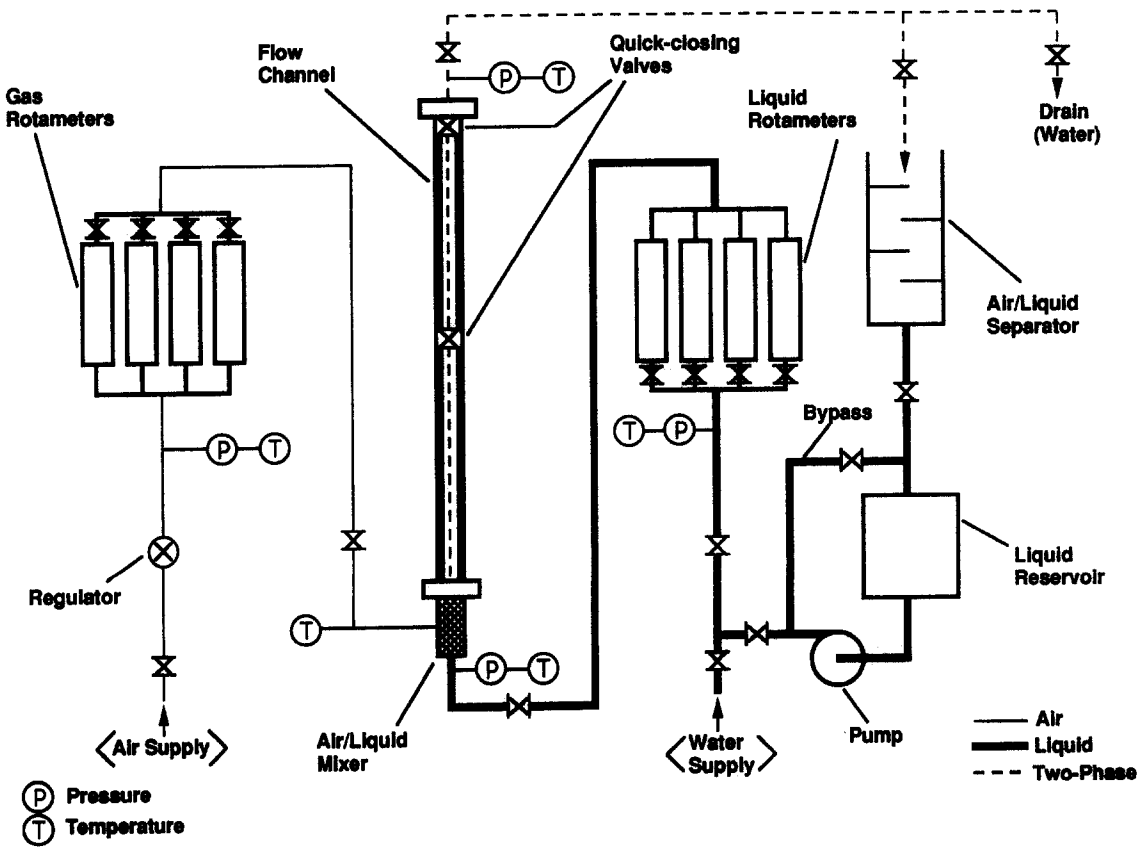

Figure 2. Schematic diagram of the experimental apparatus.

and a weighing-technique-with-stop-watch was used to calibrate the liquid rotameters. Equations were developed to fit the calibration data. The estimated uncertainty in flow rate measurement is $\pm 3\%$.

The flow channel used in the present study had a rectangular cross section of 19.05×3.18 mm and a length of 1.14 m. A channel designation, R–x–y, was used in this study, where R refers to *R*ectangular, x refers to the long dimension of the rectangle in mm and y refers to the aspect ratio. (In horizontal flow, the vertical dimension is taken as the numerator in calculating an aspect ratio.) The channel material was Plexiglas, and the flow was viewed through the long sides.

The measured dependent variable was pressure. Pressure taps were spaced at intervals of 114 mm along the entire length of the channel, at the center of the long side. Both differential pressure, over a specified channel length, and dynamic pressures, at two locations, were measured. Differential pressure was measured with a strain-gauge-type transducer (Viatran Model 209), while dynamic pressures were measured with piezoresistive-type transducers (Endevco Model 8510B-50). d.c. Drift associated with the piezoresistive-type transducers precluded their use in determining differential pressure because the need to determine a small pressure difference from the subtraction of two relatively large values gave unacceptable error. The pressure transducers were calibrated against a known standard. Relative to the exit of the mixer, the pressure taps used to measure differential pressure were centered at 718 mm ($L/D_h = 132$), while the dynamic-pressure-measuring transducers were positioned at 546 and 775 mm, L/D_h of 100 and 142, respectively. The estimated uncertainty in pressure measurements is $\pm 5\%$.

PATTERN DEFINITION

Considerable differences exist in the various researchers' definitions of two-phase flow patterns. In many instances, the definitions were not clear or comprehensive. In this study, six commonly used flow descriptors were chosen for the six basic flow patterns encountered. The descriptors were adapted from those given by Taitel & Dukler (1976), Collier (1981) and Chisholm (1983). Because flow pattern identification by visual observation is subjective, it is essential that the flow patterns be defined in detail. The descriptors used in this study are defined below:

- *Stratified.* Liquid flows along the bottom of the channel as gravity forces dominate; a smooth interface exists between the liquid and gas (no significant interfacial waves).
- *Wave.* Similar to stratified but with waves at the interface traveling in the direction of the flow; waves do not touch the upper surface of the channel. If distinct large-amplitude waves occur in the bottom film of an otherwise annular flow, the flow pattern is defined as wavy.
- *Plug.* Intermittent plugs of gas (elongated bubbles, generally varied in size), formed by many bubbles coalescing, flow in a continuous liquid phase; plugs tend to travel in the upper half of the flow channel.
- *Slug.* Intermittent slugs of liquid (typically "frothy"), formed, for example, in "wave" flow by the waves growing to touch the upper surface of the channel, propagate along the channel at high velocity; the upper surface of the channel is wetted by a residual film of liquid that drains back into bulk liquid.
- *Bubble.* Dispersed vapor distributed as discrete small bubbles (generally uniform in size) in the continuous liquid phase; bubbles tend to travel in the upper portion of the channel. With an increase in the vapor velocity, the number of bubbles grows to fill the entire channel cross section.
- *Annular (annular dispersed liquid).* Liquid forms a film around the channel periphery, with a vapor core that may contain entrained droplets; the liquid film can be expected to be thicker at the channel base. Regular film interface without surface waves (with large-amplitude waves on the bottom film, the flow pattern is classified as wavy).

RESULTS

Photographs of flow patterns obtained in this study and representative of the six different flow pattern types are given in figure 3. A typical flow pattern from each of the two separate orientations (aspect ratio >1 and <1) is shown. Key features of the patterns are observed in figure 3 according to the definitions given. Considering the aspect ratio of 6, the wave flow is seen to have distinct large-amplitude waves in what would otherwise be considered annular flow. Not all researchers make a distinction between annular and wave flow, and this difference is important when comparing results among them. The slug flow regime is characterized by froth in the flow, as shown in figure 3, while plug flow is considerably more quiescent. Bubble flow has numerous clear and relatively uniform bubbles (as opposed to plug flow). Small flow channels can suppress the bubble flow regime, and the clear bubble flows found with both aspect ratios of the small channel of this study were not accurately predictable *a priori*. (Preliminary tests with a half-scale rectangular cross section did not exhibit a bubble flow regime.)

The flow patterns were viewed from the horizontal (side) position for an aspect ratio of 6, and from the vertical (top) position for an aspect ratio of 1/6. Only four of the six flow patterns were observed for the 1/6 aspect ratio tests; in accordance with the findings of Troniewski & Ulbrich (1984), stratified and wave flow patterns were not observed for channels with aspect ratios <1 and a very small vertical dimension. The small vertical dimension (gap) does not allow the existence of finite-thickness films, which are characteristic of both stratified and wave flows. Waves on such films easily reached the upper surface, giving rise to other flow patterns. In this case, the gap dimension itself is an important parameter in addition to the aspect ratio.

Flow patterns have often been delineated on plots (maps), and a variety of axis parameters have been employed. In some cases, dimensionless coordinates that include the physical properties of the gas and liquid phases, as well as channel dimensions, were used in an attempt to obtain general applicability. However, success does not appear to have been achieved over a large parameter range. Consequently, in this study, superficial gas and liquid velocities—as proposed by Mandhane *et al.* (1974)—were used as the map coordinates.

Based on the Mandhane map for horizontal flow (Mandhane *et al.* 1974), test points were established (corresponding to a range of six different total mass velocities and selected values of the superficial gas velocity) to provide data that would cover the entire flow pattern map. The data would thereby allow identification of all of the flow pattern transition boundaries of interest. Flow pattern observations were also made at test conditions lying between the established test points. A computer program was developed to facilitate the experimental setup, including the computation of gas and liquid rotameter settings required to achieve a selected mass quality (or superficial gas velocity) for a given value of total mass flux; the developed rotameter calibration equations were used in the program.

Two-phase flow patterns and associated flow pattern transition boundaries were determined from visual observations of the two-phase flow in the transparent channel and from a series of photographs made with a strobe flash. The axial location at which the photographs were taken corresponds to an L/D_h of 153. With the procedure outlined above, a given value of total mass flux was established and the development of the various flow patterns was studied as mass quality (or superficial gas velocity) was increased.

The identification of flow pattern transition boundaries from visual observations is obviously subjective. In an attempt to develop an objective method, root-mean-square (RMS) values were calculated from the dynamic pressure–time signals and plotted as a function of mass quality. This information was subsequently correlated with flow patterns and flow pattern transition boundaries. The observed and photographed flow patterns and the associated flow pattern transition boundaries, were interpreted according to (1) changes in the mean static pressure drop in the channel and (2) characterizations of the dynamic pressure measurements.

Photographs that are representative of the flow patterns observed and that correspond to total mass fluxes of 100 and 1000 kg/m^2 s are given in figure 4 to illustrate the progression from one flow pattern to the next as the mass quality or, in effect, gas phase velocity, is increased. Based on visual observation of the flow, supplemental information from the photographs, and the flow pattern definitions given above, a preliminary flow-pattern map was developed. The final version, given in figure 4, was refined by using objective results from the pressure measurements. These results,

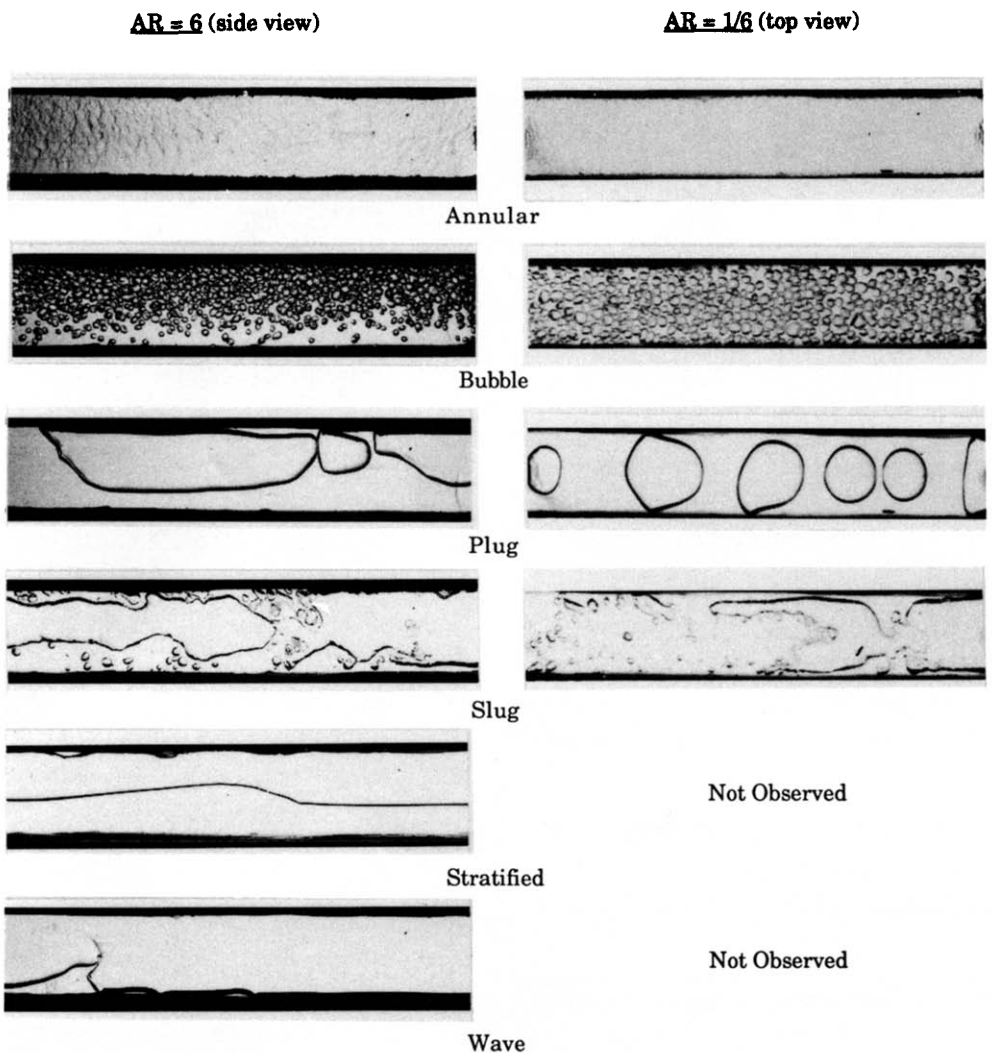

Figure 3. Flow pattern comparisons for aspect ratios of 6 and 1/6.

discussed subsequently, increased the accuracy of the determination of the transition from bubble or plug flow to slug flow. Transition boundaries delineating the stratified, wave, plug, slug, annular and bubble patterns are indicated on the map in figure 4. The test points were taken at constant values of the total mass flux. The mass flux of 100 kg/m^2 s given in figure 4 includes the plug and wave flow patterns, while the mass flux of 1000 kg/m^2 s includes the plug and bubble patterns. Differences are seen in the plug flow patterns between the two mass fluxes shown in figure 4. These patterns illustrate variations within the plug flow regime. However, both plug flow photographs conform to the pattern definition given previously and have elongated bubbles of varying sizes flowing along the top of the channel. A similar situation exists for the slug flow regimes shown in the photographs in figure 4. Frothy, intermittent slugs of liquid are present, although there is variation in slug sizes between the two mass flux situations shown.

The flow pattern maps developed for the two different orientations, viz. channels R-19.05-6 and R-19.05-0.17, are compared in figure 5. The smaller aspect ratio produced bubble flow at lower superficial liquid velocities, and the plug-to-slug flow transition occurred at higher superficial gas velocities. Although the trends of the two transitions were consistent, they were not the same as found in several other geometries, as discussed subsequently. The plug-to-slug flow transitions shown in figure 5 are well-defined and supported by pressure measurements (also discussed subsequently). The slug-to-annular flow transitions shown are more subjective. The comparison

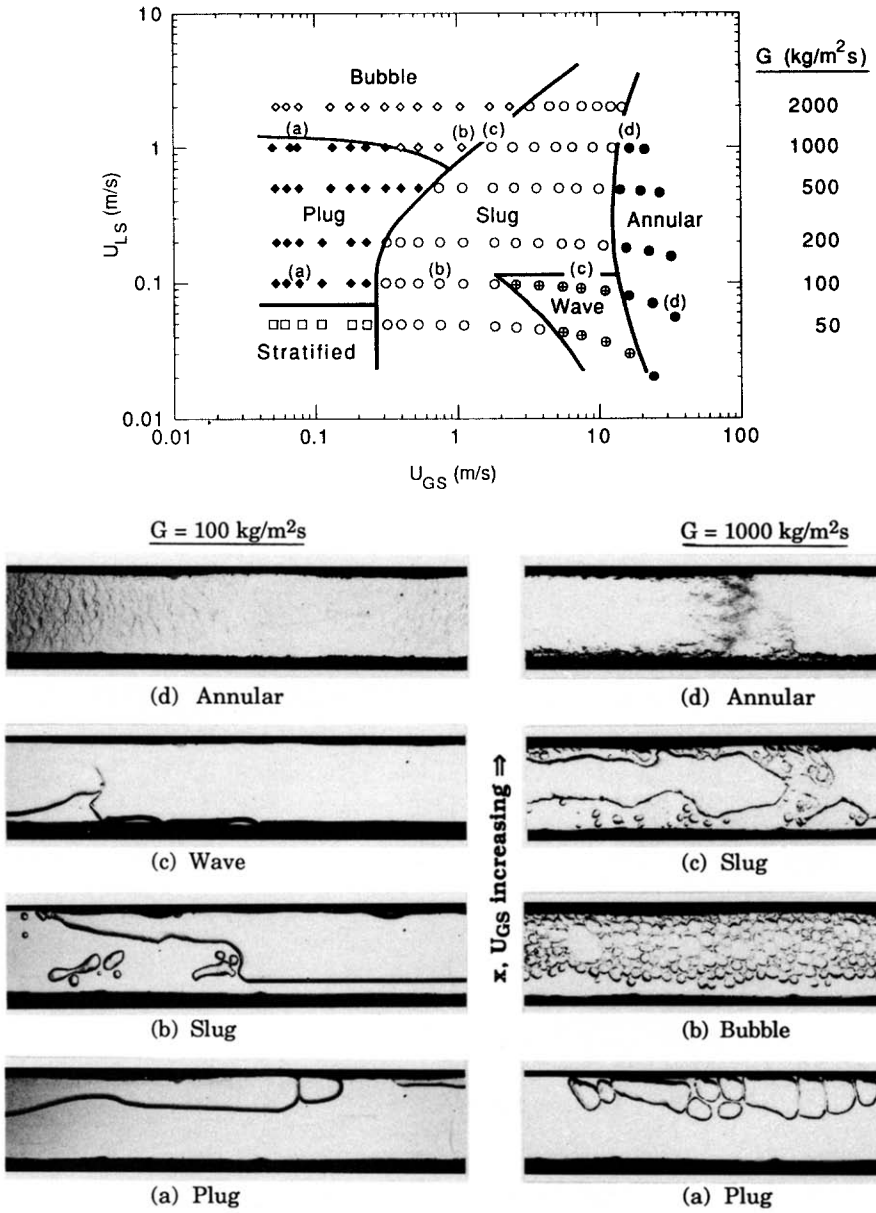

Figure 4. Flow pattern map and flow pattern development for channel R-19.05-6.

shown in figure 5 represents reasonable agreement between the two aspect ratios tested for the transition to annular flow. Researchers who did not distinguish a wave flow pattern generally interpreted the transition to annular flow according to the trend of the 1/6 aspect ratio results of the present study, where wave flow was not encountered. If wave flow was not recognized in the present aspect ratio 6 tests, the transition to an annular flow boundary would follow the 1/6 aspect ratio results.

DISCUSSION

Flow pattern transitions

The pressure-drop measurements made in the flow channel were inspected to determine if indications of flow pattern transitions were evident. In particular, the frictional pressure gradient was plotted in terms of the two-phase frictional multiplier as a function of mass quality.

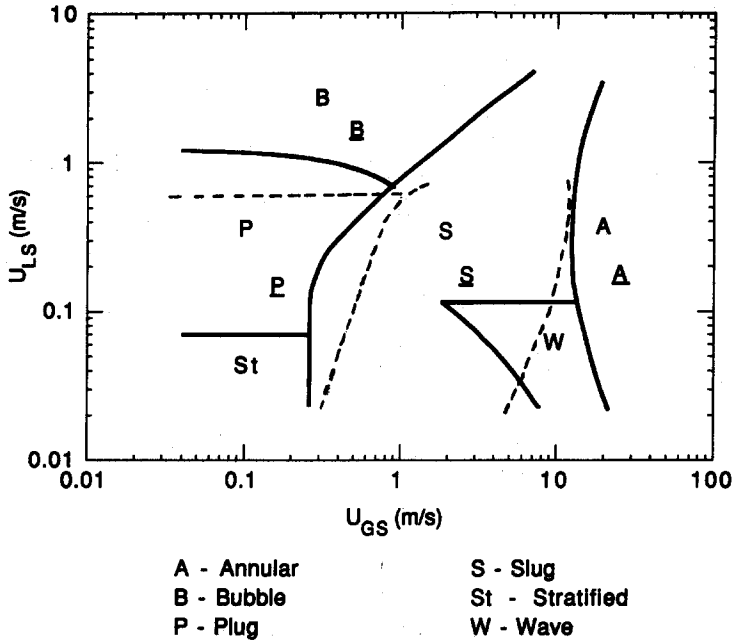

Figure 5. Superposition of two aspect ratio maps: —, AR = 6 (R-19.05-6); – – –, AR = 1/6 (R-19.05-0.17) (underlined flow pattern designations are associated with channel R-19.05-0.17 data).

A distinguishing feature was observed in the results, viz. a discontinuity in the curves at a mass quality in the range 0.002–0.008; a mass quality of 0.002 corresponds to a Martinelli parameter of approx. 10. While the discontinuity was clearly evident at all mass fluxes tested, it was most pronounced at the mass flux of 500 kg/m^2 s, shown in figure 6. When the two-phase flow patterns were considered in terms of this discontinuity, it was found to occur consistently at the plug or bubble flow transition to slug flow. It is significant that this low quality behavior in the pressure gradient has generally not been considered in models used for predicting pressure gradients in two-phase flow. The phenomenon is not unique to rectangular cross sections and was also found in a circular channel of 6.3 mm i.d. No clearly distinguishable feature was found in the two-phase friction multiplier at any other flow transition.

The results shown in figure 6 indicate that the *plug/bubble-to-slug flow transition is evident in the two-phase frictional pressure-gradient data, while the slug-to-annular transition (also slug-to-wave and wave-to-annular for the low values of mass flux) is not evident.* The transition from

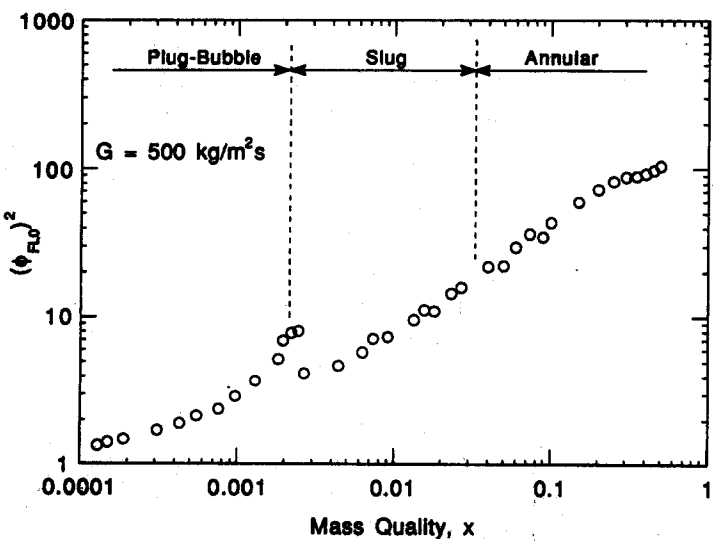

Figure 6. Pressure gradient, transition indication.

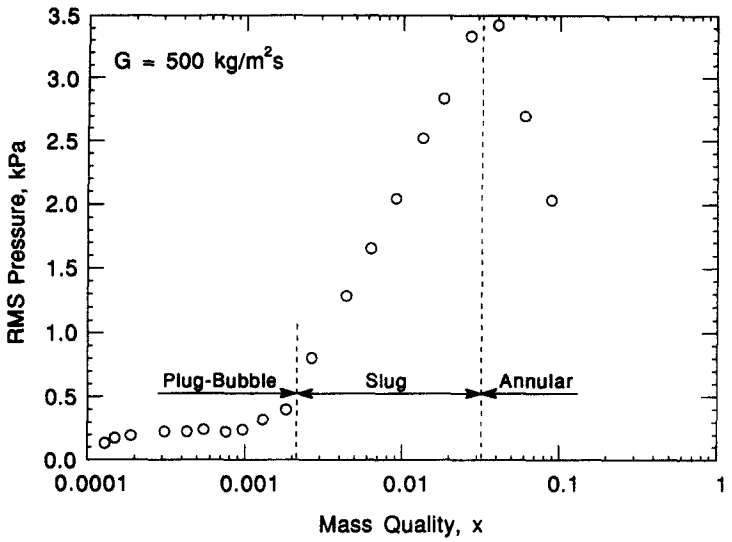

Figure 7. RMS pressure, transition indication.

plug/bubble-to-slug flow is abrupt and readily identified by visual observation of the flow patterns; this transition is also readily apparent from the series of photographs of the flow patterns (see figure 4). Conversely, the slug-to-annular transition is more gradual and is difficult to distinguish from visual observations. The former result is significant because it provides an objective means of identifying the plug/bubble-to-slug flow pattern transition from a pressure-drop measurement. It was used in establishing the transition to slug flow boundaries of the flow pattern maps in figures 4 and 5.

Several researchers (e.g. Jones & Zuber 1975; Tutu 1982; Matsui 1986; Annunziato & Girardi 1987) have attempted, with varying degrees of success, to use the pressure–time traces, or various measures (statistics) of the dynamic signals from pressure and/or void fraction measurements, to develop a methodology for identifying flow pattern transition boundaries. In this study, the RMS pressures from the dynamic pressure–time signals were used as the characteristic parameter. Plots such as figure 7 were generated, where RMS pressure was compared with observed flow pattern transitions as a function of quality.

The curve in figure 7 exhibits a well-defined breakpoint at a mass quality of approx. 0.002. This can be correlated with the discontinuity in the curve of the two-phase friction multiplier given in figure 6 and, in turn, with the transition from a plug/bubble-to-slug flow pattern. A study of the pressure-gradient results from all of the mass fluxes tested indicates a plug/bubble-to-slug flow transition occurring at an approximately constant value of quality of 0.002 for the higher mass fluxes, $G \geqslant 500$ kg/m^2 s. This result is substantiated by RMS pressure plots. At the lower mass fluxes, < 500 kg/m^2 s, the most information is derived from the RMS pressure results. These results show a change in the transition quality that is inversely proportional to mass flux. The range of transition quality of the data is $0.002 \leqslant x \leqslant 0.008$. The RMS pressure results were also used in establishing the transition to slug flow boundaries of the flow pattern maps generated in this study.

The slug-to-annular flow regime transition shown in figure 7 is very near the peak in the RMS pressure fluctuations. Considering all of the RMS data obtained at all mass fluxes it was found that the peaks correlated, approximately, with this transition. In some cases it appeared that larger amplitude fluctuations persisted at qualities beyond the slug flow regime due to intermittent regions of high concentrations of liquid drops. Here the channel appeared to be bridged, but the gas was the continuous phase. More data are required to interpret this result with greater accuracy.

Comparison with other results

The two-phase flow pattern maps developed for the small rectangular channel tested were compared with maps for large circular pipes, capillary tubes and large rectangular channels. Direct comparisons are presented in figures 8–12 for channel R-19.05-6; the results for channel R-19.05-0.17 can be inferred from these figures and figure 5. The objectives were to provide insight

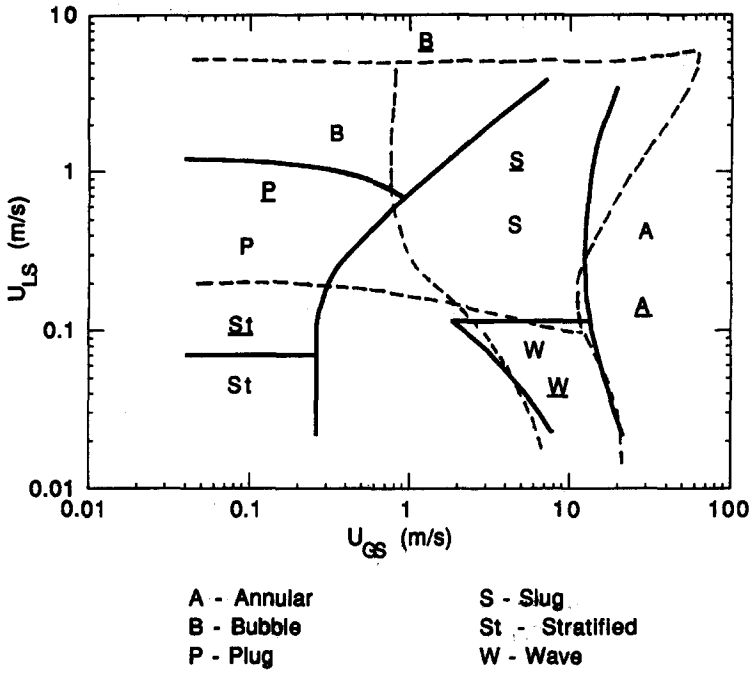

Figure 8. Comparison with the map of Mandhane *et al.* (1974): —, channel R-19.05-6; – – –, Mandhane *et al.*'s data (underlined flow pattern designations are associated with Mandhane *et al.*'s data).

relative to the effects of channel geometry and size on flow patterns and transition boundaries, and to assess the adequacy of extrapolating previous work.

In figures 8 and 9, the channel R-19.05-6 map is compared with the maps proposed by Mandhane *et al.* (1974) and Govier & Omer (1962), respectively, for circular pipes. In figures 10 and 11, the channel 19.05-6 map is compared with the recently developed maps of Damianides (1987) and Fukano *et al.* (1989), respectively, for capillary tubes of *diameter approximately equal to the hydraulic diameter of the subject channel.*

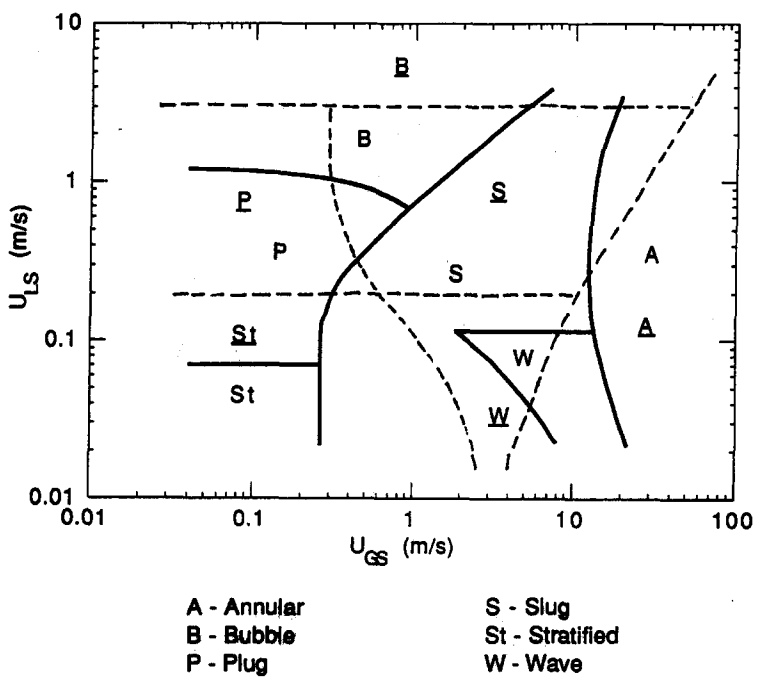

Figure 9. Comparison with the map of Govier & Omer (1962): —, channel R-19.05-6; – – –, Govier & Omer's data (underlined flow pattern designations are associated with Govier & Omer's data).

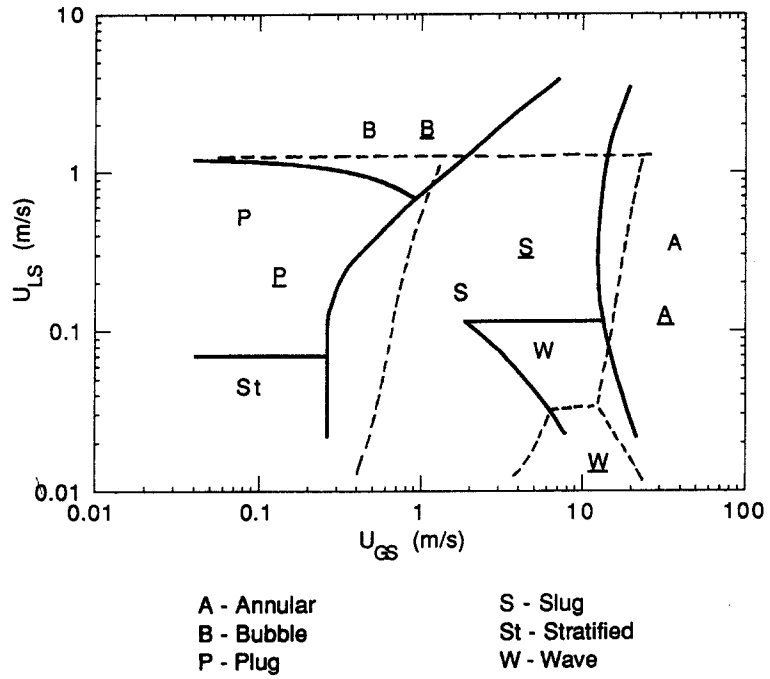

Figure 10. Comparison with the map of Damianides (1987) for a 5 mm tube: —, channel R-19.05-6; – – –, Damianides' data (underlined flow pattern designations are associated with Damianides' data).

The comparisons given in figures 8 and 9 lead to the conclusion that, while there is qualitative agreement, in general, the maps developed from data on moderate- to large-diameter pipes are not directly applicable to small, rectangular channels; an exception is the wavy flow region defined on the Mandhane map. Poor agreement is seem in the magnitude and trends of the transition to slug flow boundaries and in superficial liquid velocities at which the transition from plug to stratified flow and plug to bubble flow occurred.

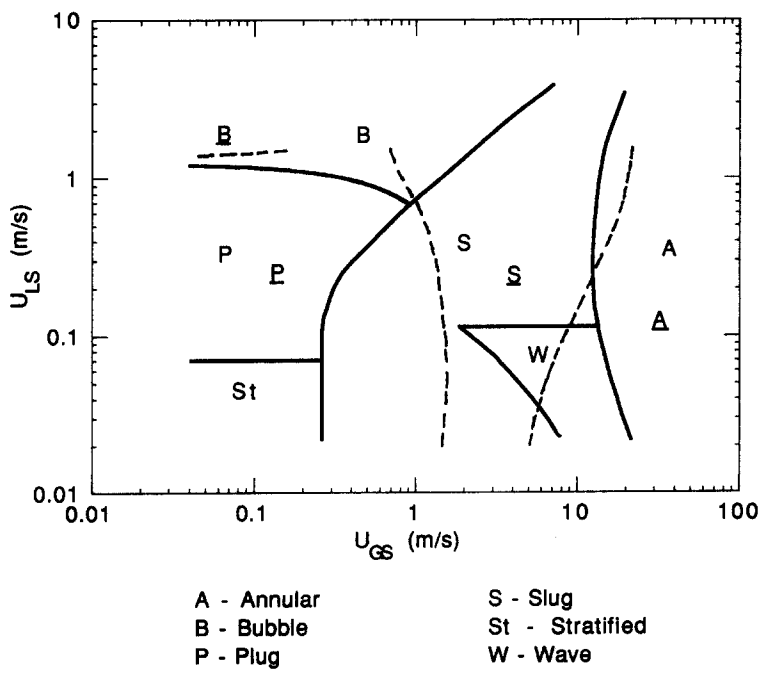

Figure 11. Comparison with the data of Fukano *et al.* (1989) for $D = 4.9$ mm tube; —, channel R-19.05-6; – – –, Fukano *et al.*'s data (underlined flow pattern designations are associated with Fukano *et al.*'s data).

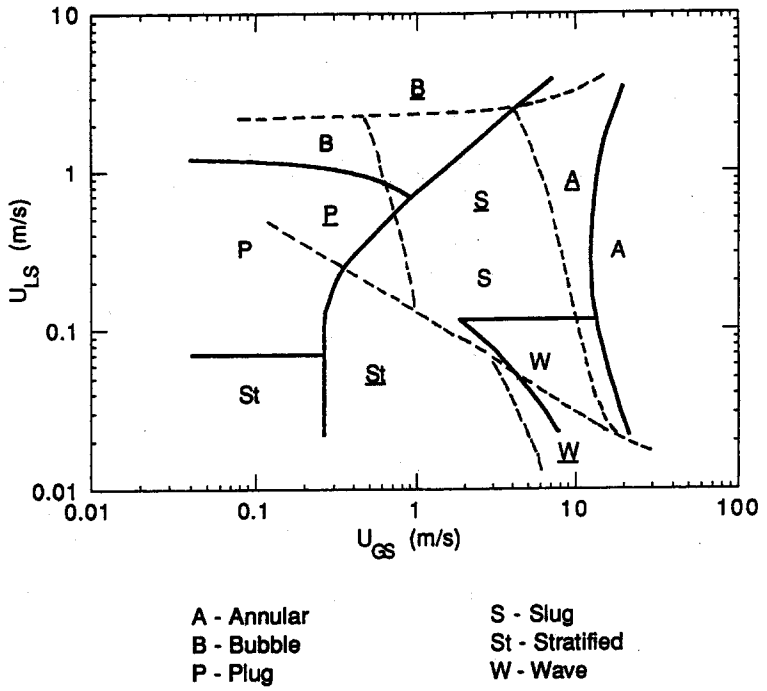

Figure 12. Comparison with the map of Troniewski & Ulbrich (1984) for horizontal, rectangular channels: —, channel R-19.05-6; – – –, Troniewski & Ulbrich's data (underlined flow pattern designations are associated with Troniewski & Ulbrich's data).

The prediction of the transition from stratified or plug flow to slug flow is not much improved by using capillary tube results, as shown in figures 10 and 11. This boundary is of particular interest because in the present study it was very well defined by a transition that was very distinct (abrupt) and, thereby, readily identifiable visually. Further, confirmation of this transition was provided by photographs and by well-defined changes in the characteristics of both the mean pressure drop and RMS pressures that have been associated with the transition. The four maps that the subject data are being compared against, figures 8–11, are all for *circular* channels. It is speculated that the poor agreement in this transition to slug flow boundary may be attributed to geometry effects; bubble formation and persistence, with increasing gas velocity, may be different in rectangular channels than in circular.

The bubble-to-plug transition is not well predicted by the maps based on large circular pipe data (figures 8 and 9), while the maps based on the capillary tube data (figures 10 and 11) are in good agreement. This result suggests that the transition may be size-dependent, as determined by hydraulic diameter, or at least not strongly dependent on geometry.

A stratified flow region was not defined for the two capillary tube flow maps. However, the stratified-to-plug transition on the large circular pipe maps (figures 8 and 9) occurs at a liquid superficial velocity 2–3 times higher than that for channel R-19.05-6. This result is similar to the bubble-to-plug transition, which also occurs at a higher liquid superficial velocity in large circular pipe flows.

As discussed earlier, of the various transitions possible, the slug-to-annular transition is perhaps the most difficult transition to identify; as a consequence, its identification is somewhat subjective. Therefore, the possibility of different interpretations by different investigators should be considered when making comparisons involving this transition boundary. With this in mind, it was observed from the four comparison plots of figures 8–11 that the slug-to-annular transition on the maps for both the circular pipe and capillary tube data are in reasonable agreement with each other, but vary from the channel R-19.05-6 data for liquid velocities above approx. 0.15 m/s. [However, the slug-to-annular flow transition for channel R-19.05-6 is in good agreement with the Fukano *et al.* (1989) data (not shown) for a 1 mm capillary tube; this single piece of evidence would suggest a possible size and/or geometry effect.] Recognizing that the physics of the flow may be different for

large and small channels it is nevertheless of interest to note that for liquid velocities below about 0.15 m/s, the slug-to-annular transition for channel R-19.05-6 is in very good agreement with the Mandhane flow pattern map (figure 8), as is the entire wave flow region, while there are discrepancies with the data of the other maps.

Specification of the wave flow region is highly dependent on the definition employed, as there can easily be overlap with the annular flow region. As a consequence, the discrepancies in the wave flow regions defined on the Govier & Omer (figure 9) and Damianides (figure 10) maps are speculated to be due largely to differences in definition/interpretation among the researchers. (This result highlights the importance of providing clear definitions of the flow pattern descriptors utilized in developing the flow pattern maps.)

It is notable that for large channels stratified flow develops into wavy flow directly, as shown in figures 8 and 9. The small channel of this study and the capillary channels of Damianides (1987), shown in figure 10, exhibit a slug flow regime between stratified and wavy. It was observed in the present study that the appearance of small-amplitude surface waves in a stratified flow almost immediately reached the top wall of the channel producing a relatively quiescent slug flow with little froth, as shown in figure 4(b) at $G = 100\ \text{kg/m}^2\,\text{s}$. Results for the large channels indicate that the waves do not reach the top of the channel and slug flow is not formed from stratified flow.

In the present study, increasing quality produced more froth in the slug flow, similar to the high mass flux results of figure 4(c) at $G = 1000\ \text{kg/m}^2\,\text{s}$. At yet higher qualities, the liquid bridges broke down and the flow moved towards the annular regime, where surface waves persisted without reaching the top of the channel, as shown in figure 4(c) at $G = 100\ \text{kg/m}^2\,\text{s}$. At higher qualities the amplitude of the waves diminished and the flow became annular. The flow regime at qualities just below annular with distinct surface waves on the bottom liquid film of the channel has been defined as wave flow. In large channels wave flow persists all the way to the low qualities of stratified flow, while the small geometry of this study produced a slug flow over the quality region just above the stratified flow regime.

Troniewski & Ulbrich (1984) developed a generalized flow pattern map for horizontal rectangular channels based on experiments with rectangular channels of various aspect ratios (see table 1). The authors plotted their map on non-dimensional coordinates with a correction factor to account for channel geometry (aspect ratio) effects; the correction was derived from analysis of a single-phase flow in rectangular channels. In figure 12, the map was transformed to superficial velocity coordinates (assuming $v_G = 0.750\ \text{m}^3/\text{kg}$ and $v_L = 0.001\ \text{m}^3/\text{kg}$) to facilitate comparison with the channel R-19.05-6 map. As one can observe from figure 12, the agreement is not good.

CONCLUSIONS

General qualitative agreement was found between two-phase flow pattern maps encountered in the small rectangular channel of the present study and larger circular channels and comparable small circular channels. However, quantitative agreement was not good in either case over all flow regimes.

The small channel dimensions did not suppress bubble flow, which was clearly achievable in both aspect ratios tested, and the transition to plug flow was in agreement with small circular channel results. Deviations from large channel results, circular and rectangular, were attributed to channel size effects.

The transition to slug flow was the best defined experimentally. Visual and photographic results were substantiated by mean and dynamic pressure measurements but were not in good agreement with any other channel data. (It was found that both pressure measurements serve as accurate indicators of this flow transition. Both of these indicators were developed as part of this investigation.) As a result, geometry effects were considered important in this region.

Discrepancies existed for the transition from slug to annular flow between the present data and data from circular tubes and larger rectangular channels. This transition was difficult to define precisely. Considering this situation for lower liquid velocities, deviations from the other data were generally attributed to the definitions of wave flow. Comparison of the present study results with

those of Mandhane *et al.* (1974) was a notable exception, showing excellent agreement in the entire wave flow region.

The data from the small rectangular channel of the present study were in poor agreement with the generalized rectangular two-phase flow pattern results of Troniewski & Ulbrich (1984), which were based on larger channels. Also, only sporadic agreement was obtained with these small rectangular channel data and results from circular channels, large or small. At this time, flow pattern transitions in small rectangular channels are best determined independently.

Acknowledgments—The authors thank Drs K. J. Bell, C. B. Panchal and N. T. Obot of Argonne National Laboratory for their many and varied contributions throughout this research activity. The authors also thank Mr R. K. Smith and Ms J. A. Stephens for their important contributions to this effort.

The research is funded by the U.S. Department of Energy, Office of Conservation and Renewable Energy, Division of Advanced Industrial Concepts, and represents a U.S. contribution to the International Energy Agency (IEA) program on Research and Development in Heat Transfer and Heat Exchangers.

REFERENCES

ANNUNZIATO, M. & GIRARDI, G. 1987 Horizontal two phase flow: a statistical method for flow pattern recognition. In *Proc. 3rd Int. Conf. on Multiphase Flow*, The Hague, The Netherlands, Paper F1, 169–185.

BELL, K. J. 1988 Two-phase flow regime considerations in condenser and vaporizer design. *Int. Commun. Heat Mass Transfer* **15,** 429–448.

CHISHOLM, D. 1983 *Two-phase Flow in Pipelines and Heat Exchangers.* George Godwin, London.

COLLIER, J. G. 1981 *Convective Boiling and Condensation*, 2nd edn. McGraw-Hill, New York.

DAMIANIDES, C. A. 1987 Horizontal two-phase flow of air–water mixtures in small diameter tubes and compact heat exchangers. Ph.D. Dissertation, Univ. of Illinois at Urbana-Champaign.

FUKANO, T., KARIYASAKI, A. & KAGAWA, M. 1989 Flow patterns and pressure drop in isothermal gas–liquid concurrent flow in a horizontal capillary tube. *ANS Proc. 1989 Natn. Heat Transfer Conf.* **4,** 153–161.

GOVIER, G. W. & OMER, M. M. 1962 Horizontal pipeflow of air–water mixtures. *Can. J. chem. Engng* **40,** 93–104.

HOSLER, E. R. 1968 Flow patterns in high pressure two-phase (steam–water) flow with heat addition. *AIChE Symp. Ser.* **64,** 54–66.

JONES, O. C. JR & ZUBER, N. 1975 The interrelation between void fraction fluctuations and flow patterns in two-phase flow. *Int. J. Multiphase Flow* **2,** 273–306.

LOWRY, B. & KAWAJI, M. 1988 Adiabatic vertical two-phase flow in narrow flow channels. *AIChE Symp. Ser.* **84,** 133–139.

MANDHANE, J. M., GREGORY, C. A. & AZIZ, K. 1974 A flow pattern map for gas–liquid flow in horizontal pipes. *Int. J. Multiphase Flow* **1,** 537–554.

MATSUI, G. 1986 Automatic identification of flow regimes in vertical two-phase flow using differential pressure fluctuations. *Nucl. Engng Des.* **95,** 221–231.

RICHARDSON, B. L. 1958 Some problems in horizontal two-phase two-component flow. Argonne National Lab. Report ANL-5949.

SHAH, R. K. 1982 Advances in compact heat exchanger technology and design theory. In *Heat Transfer 1982*, Vol. 2, pp. 123–142. Hemisphere, Washington, D.C.

TAITEL, Y. & DUKLER, A. E. 1976 A model for predicting flow regime transitions in horizontal and near horizontal gas–liquid flow. *AIChE Jl* **22,** 47–55.

TAITEL, Y., BARNEA, D. & DUKLER, A. E. 1980 Modelling flow pattern transitions for steady upward gas–liquid flow in vertical tubes. *AIChE Jl* **26,** 345–354.

TRONIEWSKI, L. & ULBRICH, R. 1984 Two-phase gas–liquid flow in rectangular channels. *Chem. Engng Sci.* **39,** 751–765.

TUTU, N. K. 1982 Pressure fluctuations and flow pattern recognition in vertical two phase gas–liquid flows. *Int. J. Multiphase Flow* **8,** 443–447.

WAMBSGANSS, M. W., JENDRZEJCZYK, J. A., FRANCE, D. M. & OBOT, N. T. 1990 Two-phase flow patterns and frictional pressure gradients in a small, horizontal, rectangular channel. Argonne National Lab. Report ANL-90/19.

WESTWATER, J. W. 1986 Compact heat exchangers with phase change. *Proc. 8th Int. Heat Transfer Conf.* **1**, 269–278.